ELSEVIER

Journal of Power Sources 68 (1997) 565–569

JOURNAL OF POWER SOURCES

Influence of morphology on the stability of $LiNiO_2$

W. Li *, J.C. Currie, J. Wolstenholme

Westaim Corporation 10102-114 St. Fort Saskatchewan, Alta., T8L 3W4, Canada

Accepted 21 August 1996

Abstract

$LiCoO_2$ is currently used as a cathode material in most commercial lithium-ion batteries. Lithium intercalation compounds such as $LiNiO_2$ are being pursued as lower cost alternatives to $LiCoO_2$. Although cathodes of $LiNiO_2$ provide higher capacity at a lower cost the layered structure becomes unstable during the cell charging process as the material is delithiated. The instability of $LiNiO_2$ in lithium-ion cells reduces the cycle life of the cell and leads to safety concerns. In this paper we determine the influence of particle size and particle morphology on the thermal stability of lithiated $LiNiO_2$. Five different particle size (P_c) cathode materials were prepared by a proprietary Westaim process and the thermal and electrochemical stability determined. Thermogravimetric analysis indicates that the thermal stability of $LiNiO_2$ depends on P_c, not on the particle size of the agglomerate (P_a). $LiNiO_2$ with a large P_c is more thermally stable than those with a small P_c. The $LiNiO_2$ cathode material exhibits a reversible electrochemical capacity of about 150 mAh/g when tested in an Li/$LiNiO_2$ cell. The $LiNiO_2$ cathode material with a large P_c has a slightly lower reversible capacity than that with a small P_c. © 1997 Elsevier Science S.A.

Keywords: Lithium-ion batteries; Cathodes; Lithium nickel dioxide; Stability; Morphology

1. Introduction

The dramatic growth of the portable electronic device market has placed an increased demand on the availability and performance of rechargeable batteries. New battery technologies have been developed and existing systems improved to meet the demanding performance requirements of portable appliances. In the early 1990's Sony introduced a rechargeable Li-ion battery with a lithium cobalt dioxide cathode and a carbon anode [1]. The battery operates at an average discharge voltage of 3.6 V, the highest voltage among commercial rechargeable batteries. The high cost and moderate reversible capacity of the cobalt-based lithium-ion system has prompted the development of lower cost cathode materials such $LiNiO_2$ [2] and $LiMn_2O_4$ [3]. The latter has a reversible capacity between 100 and 140 mAh/g but a high fade rate at the higher capacities [4,5]. Although, $LiNiO_2$ has a much higher reversible capacity of about 200 mAh/g, it also has a high fade rate [6].

This paper addresses the influence of particle morphology on the electrochemical properties and thermal stability of $LiNiO_2$ powders. The electrochemical behavior of these intercalation electrode materials is strongly influenced by their lattice structure as well as the particle size and surface area. For example, when lithium is intercalated or de-intercalated in Li_xNiO_2, a series of phase transitions appear [7–9] which affect its structural stability. Although $LiNiO_2$ has a high capacity, its stability needs to be improved for it to have widespread use in commercial batteries. The fully lithiated cathode material, $LiNiO_2$, is stable, but becomes destabilized as lithium is removed from the host lattice during the charge cycle. At moderate temperatures, Li_xNiO_2 with a low value of x is able to release oxygen which can react with the electrolyte to generate heat and accelerate further decomposition of the cell components [10]. Thermogravimetric analysis has shown that the order of increasing thermal stability among the delithiated lithium-ion battery materials is $Li_{0.3}NiO_2$, $Li_{0.4}CoO_2$ and $Li_{0.0}Mn_2O_4$ [11], and the stabilities of $LiNiO_2$ and $LiCoO_2$ depend on how much of the lithium is de-intercalated. The relation between the stability and the particle size of the materials has not been addressed.

In our experience, $LiCoO_2$ is easy to prepare with various crystal sizes P_c. However, it is much more difficult to make large single crystals of $LiNiO_2$. To our knowledge, there is no report of $LiNiO_2$ materials with P_c larger than 5 μm, although $LiNiO_2$ can be made with a large agglomerate sizes P_a [12].

In the present study, we have made $LiNiO_2$ with various crystal sizes, P_c, and surface areas by using proprietary Westaim technology; P_c is in the range 1 to 20 μm. A low surface

* Corresponding author.

PII S0378-7753(96)02566-9

area of $LiNiO_2$ is preferred [13] to minimize the contact area between $LiNiO_2$ and the electrolyte from a standpoint of chemical reactivity. We have made $LiNiO_2$ with a surface area as low as 0.2 m^2/g. Thermogravimetric analysis indicates that $LiNiO_2$ with a large P_c is more stable than that with a small P_c, and that agglomerated $LiNiO_2$ with a large P_a and a small P_c does not exhibit high thermal stability compared to $LiNiO_2$ with a large P_c. The thermal stability does not appear to be directly dependent on surface area. Materials with various crystal particle sizes (P_c) exhibit slightly different reversible capacities.

2. Experimental

$LiNiO_2$ was prepared by a proprietary Westaim process. The cell cathode consists of $LiNiO_2$ powders mixed with an 8% w/w Super S carbon black and a 2% w/w of EPDM (ethylenepropylenediene terpolymer) binder to make a slurry in cyclohexane. The mixture was spread on an aluminum foil and dried at room temperature. Cathodes of 1.2 cm × 1.2 cm usually contained 20 mg/cm^2 of active material. 1 M $LiBF_4$ in PC/EC/DMC (25:25:50) was used as the electrolyte. A 2325 coin cell was assembled in a glove box filled with ultra-pure argon. An Arbin battery tester model 2042 controlled the cell during cycling tests.

X-ray diffraction (XRD) was measured on a Siemens diffractometer 5000 with Cu $K\alpha_1$ and $K\alpha_2$ as X-ray sources. A Cahn TG 171 was used for thermogravimetric analysis (TGA). Particle size was determined on a Microtrac X100 particle analyzer based on light scattering principles. Both scanning electronic microscope (SEM) and the Microtrac were required to distinguish the values of P_a and P_c. For $P_a = P_c$, each particle is essentially composed of one crystal, and for $P_a > P_c$ each particle is an agglomerate of small crystals. We report P_a and P_c based on the average particle size. BET (Brunnaurer–Emmett–Teller) surface area was measured on a Monosorb apparatus from Quanta Chrome.

3. Results

Fig. 1 shows a typical XRD pattern of the $LiNiO_2$ prepared by our proprietary process. Fig. 1(a) gives XRD data at scattering angles between 15° and 90°, and Fig. 1(b) shows the peaks at low angles from 35° to 50°. The lattice constants, $a = 2.877$ Å and $b = 14.18$ Å were determined. In Fig. 1(b), the splitting due to the X-ray wavelength difference of Cu $K\alpha_1$ and Cu $K\alpha_2$ in peaks 006, 102, 104 and 105 are observed at scattering angles 38.0°, 38.3°, 44.5° and 48.6°, respectively, and the sharp peaks have a narrow full width at half-maximum intensity (FWHM). The perfect atom ratio of Li/Ni = 1:1 for $LiNiO_2$ is difficult to obtain; therefore, the formula for our material can be written as $Li_xNi_{2-x}O_2$. If the samples are not uniform, the splitting cannot be observed at low angles because lattice constants depend on the value of x in

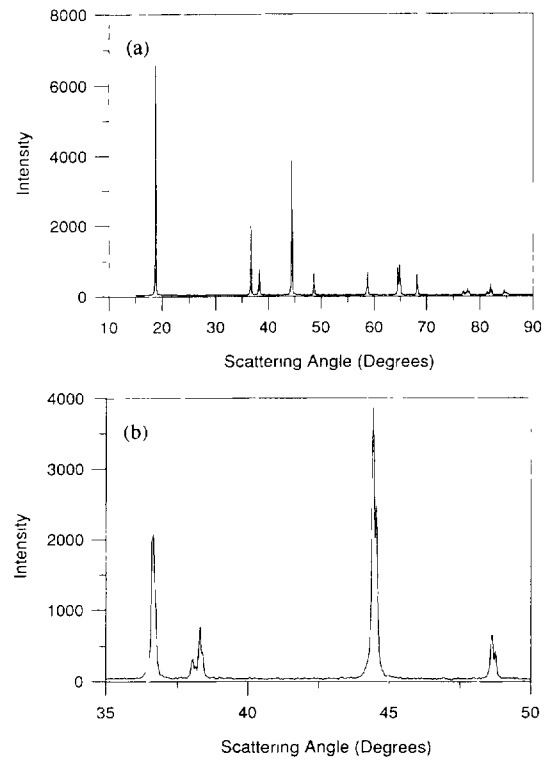

Fig. 1. The X-ray diffraction showing a typical $LiNiO_2$ material made in Westaim (a) The X-ray diffraction from 15° to 90° (b) The X-ray diffraction from 35° to 50°.

$Li_xNi_{2-x}O_2$ [7]. Furthermore, the splitting cannot be observed at low angles for the samples with a low crystallinity because only long-range order in a lattice ensures a small FWHM. Therefore, our samples are uniform and highly crystalline.

The stoichiometry of x in $Li_xNi_{2-x}O_2$, was determined by X-ray analysis and titration. The ratio of the X-ray Bragg intensities is defined as

$$R = (I(006) + I(102))/I(101) \quad (1)$$

For a perfect layered structure with $x = 1$ the value of R is 0.411 [14]. In our samples, the value of R is 0.427 which means x is 0.994. By the titration method, the total nickel content was determined by EDTA titration, and the Ni(III) content was determined by a method of reduction of Ni(III) to Ni(II) with excess ferrous ammonium sulfate followed by back titration with standard potassium dichromate. This method indicates that 99% of the nickel in $LiNiO_2$ is present as Ni(III) which is consistent with the X-ray result.

Fig. 2 shows the SEM graphs of three samples with various particle sizes P_c and P_a. The top SEM is of JEC #6 sample made by Honjo Chemical with a P_a of about 20 μm, but a P_c of less than 1 μm. Two samples of $LiNiO_2$ made by the Westaim process are shown in the middle and the bottom of Fig. 2. The first Westaim sample has a P_a of about 8 μm and a crystal size P_c of about 4 μm, and in the second sample both P_a and P_c are about 12 μm. According to our results, the thermal stability between these samples is significantly different due to the difference in P_c.

Fig. 2 The scanning electron micrographs of three samples of $LiNiO_2$ with various P_a and P_c values. The top micrograph is the JEC#6 sample and bottom samples are Westaim materials. All of the micrographs are magnified 3500 times and the dimension bar is 5 μm.

When $LiNiO_2$ was heated to high temperatures in the absence of oxygen the following reaction is expected:

$$2LiNiO_2 \rightarrow Li_2O + 2NiO + 1/2O_2 \quad (2)$$

If reaction (2) is complete, a weight loss of 8.1% due to the loss of oxygen is observed. If reaction (2) is incomplete, the final products of the reaction may be $Li_xNi_{2-x}O_2$ ($0<x<1$), Li_2O and O_2, and the weight loss will be less than 8.1%. On the other hand, if the value of x for the starting material is less than 1 then the weight loss will be less than that of a fully lithiated starting material.

In battery applications, the instability of $Li_{1-y}NiO_2$ ($0.5<y<1.0$) may lead to unsafe operation of the battery. As a first step in a series of studies on the stability of lithium-ion cathode materials we determined the thermal stability of fully lithiated $LiNiO_2$ with various crystal and agglomerate sizes. The thermal stability of $LiNiO_2$ was measured by heating the samples from room temperature to 1000 °C at 4 °C/min or at 8 °C/min under an argon atmosphere. The initial sample size is about 445 mg for all samples. Fig. 3(a) shows the weight loss of three $LiNiO_2$ samples (solid lines) between 500 and 900 °C. The three samples are #2, #3 and JEC#6, corresponding to P_c values of 13.0, 5.5 and 1 μm, respectively. The least stable sample is JEC#6 with a P_c value of 1 μm and the most stable sample is #2 with a P_c value of 13.0 μm. By comparison, an $LiCoO_2$ sample (dashed line) does not experience significant weight loss.

Fig. 3(b) shows the temperature, T_c, at which a significant weight loss starts for samples with various P_c values. The open triangles and the black triangles represent onset T_c values measured at two heating rates, 8 and 4 °C/min, respectively. Clearly, $LiNiO_2$ with a larger P_c value decomposes at higher temperatures. However $LiNiO_2$ with a large P_a is unstable. Table 1 summarizes the T_c data for six samples of $LiNiO_2$. The samples include #1 to #5 prepared in Westaim and a sample from JEC, #6. In order to rule out the effects of the lattice structure which may change T_c, we also list the

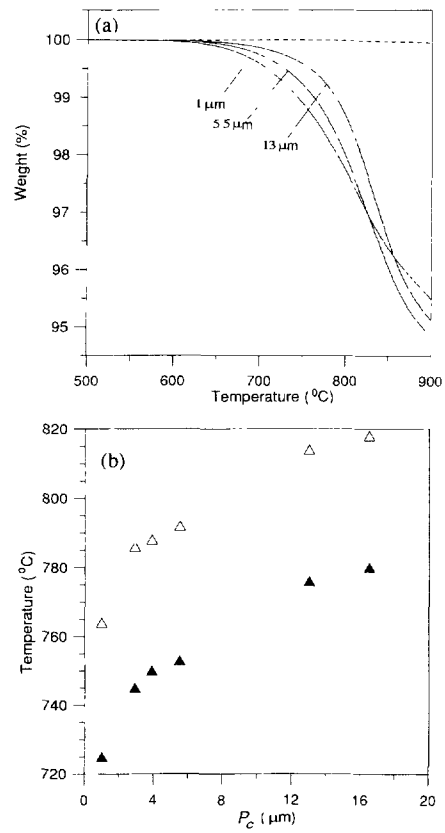

Fig. 3 The TGA data of $LiNiO_2$ with various P_c values (a) The weight loss versus the temperature for three $LiNiO_2$ samples (solid lines) with various P_c. A $LiCoO_2$ sample (dash line) is also illustrated. The temperature was increased at 4 °C/min. (b) the particle size P_c versus the onset temperature, T_c, at which $LiNiO_2$ starts to decompose. The open triangles were measured at temperature increasing at 8 °C/min and the black triangles were measured at temperature increasing at 4 °C/min

Table 1
Summary of thermal and electrochemical behaviors of $LiNiO_2$

Sample no	1	2	3	4	5	JEC #6
P_c (μm)	16 5	13.0	5 5	3.9	2.9	1
P_a (μm)	16.5	13 0	8 3	5.1	5.8	20.0
a (Å)	2.8765	2.8763	2.8739	2.8740	2.8769	2.8811
b (Å)	14.1856	14 1893	14.1833	14.1837	14.1918	14.2020
T_c, 4 °C/min (°C)	780	776	753	750	745	725
T_c, 8 °C/min (°C)	818	814	792	788	786	764
Capacity mAh/g (3.0–4.15 V)	139	145	143	150	150	139
Surface area (m^2/g)	0 19	0.32	1.7	2.1	1.5	0.42

lattice constants a and b of $LiNiO_2$ in Table 1. Because the actual material does not have a perfect Li:Ni ratio of 1.0:1.0, and since the lattice constants are correlated with x in $Li_xNi_{2-x}O_2$ [7], the lattice constants are used to identify the lattice structure of the materials. The lattice constants a and b of sample 1 to 5 are almost identical, and the differences are within the experimental errors, but the T_c values are markedly different. This indicates that the stability of $LiNiO_2$ can be partially controlled by the crystallite size and not by the agglomerate size.

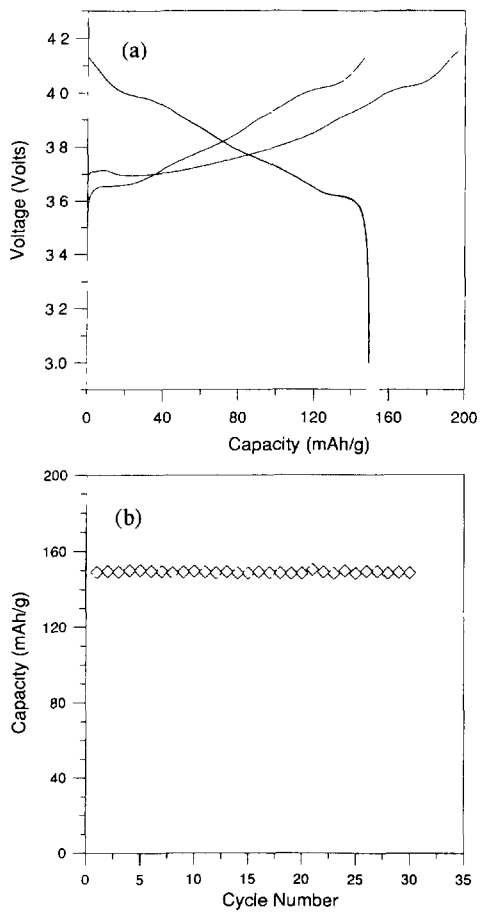

Fig. 4. The electrochemical data for a Li/$LiNiO_2$ cell with 1 M $LiBF_4$ in PC/EC/DMC (25.25:50) as an electrolyte. (a) The voltage curves for the first two charge and the first two discharge between 3.0 V and 4.15 V. (b) The cycling performance between 3.0 V and 4.15 V.

The cross over of the weight loss curve between the JEC#6 sample and the samples #2 and #3 as shown in Fig. 3(a) may be related to different values of x in $Li_xNi_{2-x}O_2$ for the three samples. The lattice parameters, a and b, for sample JEC#6 are larger than for samples #2 and #3, therefore the value of x in $Li_xNi_{2-x}O_2$ is expected to be smaller and the total weight loss is expected to be less for the former.

Fig. 4 illustrates the electrochemical performance of a typical $LiNiO_2$ material made by our Westaim process. Fig. 4(a) shows the first two charge and the first two discharge curves in an $LiNiO_2$/Li 2325 coin cell with 1 M $LiBF_4$ in PC/EC/DMC (25:25:50) as the electrolyte. The discharge current density is 0.25 mA/cm^2. The first charge capacity is about 195 mAh/g and the reversible discharge capacity is 150 mAh/g. The coulombic efficiency of the first cycle is 77% and subsequent cycles is close to 100%. The discharge curves for the first two cycles overlap, indicating stable cycle life of the cell materials. The fade rate curve described in Fig. 4(b) has a capacity fade of about 1% in the first 30 cycles, corresponding to about 0.03% capacity loss per cycle. Table 1 also lists the reversible capacities of $LiNiO_2$ samples with various crystal sizes P_c. The samples with small P_c values exhibit a slightly higher capacity than those electrodes made with large P_c values. This difference may be related to the higher rate capabilities of high surface area material and to variabilities of electrode manufacturing and cell assembly.

4. Conclusions

$LiNiO_2$ powder with large crystal sizes have been prepared. The structure of the large crystals agreed with the splitting between the X-ray Cu $K\alpha_1$ and Cu $K\alpha_2$ at low peak angles. XRD also indicated that the $LiNiO_2$ crystals prepared by the proprietary process exhibited uniform and well-developed layered structure. TGA results show that the thermal stability of large crystal $LiNiO_2$ is greater than the stability of large agglomerates of small crystals. The electrochemical experiments showed that small $LiNiO_2$ particles have a slightly higher capacity than large particle material. Although large particles of $LiNiO_2$ provide higher thermal stability, the irreversible capacity of $LiNiO_2$ should be reduced to match the irreversible capacity of carbon anodes normally used in the commercial Li-ion batteries.

References

[1] T Nagaura and K. Tozawa, *Prog. Batteries Solar Cells, 9* (1991) 209.
[2] J R. Dahn, U von Sacken, M W. Juzkow and H. Al-Janaby, *J. Electrochem. Soc., 138* (1991) 2207
[3] J.M. Tarascon and D. Guyomard, *Electrochimica Acta, 38* (1993) 1221.
[4] R.J. Gummow, A de Kock and M.M. Thackeray, *Solid State Ionics, 69* (1994) 59.
[5] Yuan Gao and J.R. Dahn, *J. Electrochem. Soc., 143* (1996) 1783
[6] S. Yamada, M Fujiwara and M. Kanda, *J. Power Sources, 54* (1995) 209.
[7] W. Li, J.N. Reimers and J.R. Dahn, *Phys. Rev. B, 46* (1992) 3236
[8] W. Li, J.N. Reimers and J.R. Dahn, *Solid State Ionics, 67* (1993) 123.
[9] T. Ohzuku, A. Ueda and M. Nagayama, *J. Electrochem. Soc., 140* (1993) 1862
[10] D. Wainwright, *J. Power Sources, 54* (1995) 192.
[11] J.R. Dahn, E.W. Fuller, M. Obrovac and U von Sacken, *Solid State Ionics, 69* (1994) 265.
[12] M. Broussely, F. Perton, P. Biensan, J.M. Bodet, J. Labat, A. Lecerf, C. Delmas, A. Rougier and J.P Pérès, *J. Power Sources, 54* (1995) 109.
[13] J.R. Dahn, R. Fong and U. von Sacken, *US Patent No 5 264 201* (1993).
[14] J.N Reimers, J.R. Dahn, J.E. Greedan, C.V. Stager, G. Liu, I. Davidson and U. von Sacken, *J. Solid State Chem., 102* (1993) 542